

## Supporting information

### **Cube-like anatase TiO<sub>2</sub> single crystal with enhanced photocatalytic**

### **CO<sub>2</sub> reduction activity**

Quanlong Xu,<sup>a</sup> Jiaguo Yu,<sup>\*a,c</sup> Jun Zhang,<sup>a</sup> Jinfeng Zhang<sup>a</sup> and Gang Liu<sup>\*b</sup>

*<sup>a</sup>State Key Laboratory of Advanced Technology for Materials Synthesis and Processing, Wuhan University of Technology, Wuhan, 430070, P. R. China. E-mail: jiaguoyu@yahoo.com*

*<sup>b</sup>National Center for Nanoscience and Technology, Beijing, 100190, China. E-mail:*

*liug@nanoctr.cn*

*<sup>c</sup>Department of Physics, Faculty of Science, King Abdulaziz University, Jeddah*

*21589, Saudi Arabia*

## **Experimental details**

**Materials.** Commercially available Degussa TiO<sub>2</sub> powder (P25) was used reference. All reagents used in the experiment were of analytical grade and used as received without further purification. Deionized (DI) water was used during the whole process.

**Synthesis of single crystal TiO<sub>2</sub> cube.** Single crystal TiO<sub>2</sub> sample was synthesized using modified hydrothermal method as described in the literature (Adv. Funct. Mater., 2011, 21, 3554-3563.). In brief, 0.5 mL of [bmin][BF<sub>4</sub>], 20 mL of HAc, and 1.25 mL of water were mixed in a dried Teflon autoclave with a capacity of 50 mL under stirring at room temperature for 30 min until homogenous. Subsequently, 0.5 mL of TTIP was added into the homogenous solution and then kept at 200 °C for 24 h. After cooling naturally, the resultant pale precipitates were separated by centrifugation and washed with water several times, dried at 80 °C overnight. The dried sample was calcined in air at 550 °C for 2 h with a heating ramp of 5 °C min<sup>-1</sup>. The calcined sample was denoted TC. TW sample was also prepared in similar with preparing TW sample except for the adding of [bmin][BF<sub>4</sub>].

**Characterization.** The phase structures of the obtained samples were determined on a D/MAX-RB X-ray diffractometer (Rigaku, Japan) using Cu K $\alpha$  radiation source ( $\lambda=1.54056$  Å) at a scan rate of  $0.05^\circ 2\theta \text{ s}^{-1}$ . The accelerating voltage and the applied current were 40 kV and 80 mA, respectively. The average crystallite sizes were calculated using the Scherrer formula ( $d = K\lambda/\beta\cos \theta$ , where  $d$ ,  $\lambda$ ,  $B$ , and  $\theta$  are the crystallite size, Cu K $\alpha$  wavelength, full width at half-maximum intensity (FWHM) in radians, and Bragg's diffraction angle, respectively). Field emission scanning electron microscopy (FE-SEM) was characterized by S-4800 (Hitachi, Japan) operating at 10 kV. Transmission electron microscopy (TEM) and high-resolution transmission electron microscopy (HRTEM) were conducted on a JEM-2100F electron microscopy (JEOL, Japan) operating at 200 kV. The Brunauer-Emmett-Teller (BET) specific surface area ( $S_{\text{BET}}$ ) was analyzed by nitrogen adsorption using a Micromeritics ASAP

2020 nitrogen adsorption apparatus (USA). The BET surface area determined by a multipoint BET method using the adsorption data in the relative pressure ( $P/P_0$ ) range of 0.05-0.3. All samples used in the BET surface area were pretreated at 150 °C for 4 h. X-ray photoelectron spectroscopy (XPS) data were obtained using an ESCALab 250 Xi electron spectrometer from Thermo Scientific Corporation. Monochromatic 150 W Al K $\alpha$  radiation was utilized with a pass energy of 20 eV. Low-energy electrons were used for charge compensation. The binding energies were referenced to the adventitious C1s line at 284.8 eV. The diffuse reflectance spectra (DRS) were obtained by a UV-visible spectrometer (UV 2550, Shimadzu, Japan) equipped with an integrating sphere using BaSO $_4$  as a reference, and the optical absorptions were converted from the reflection spectra according to the Kubelka-Munk equation.

**CO $_2$  Photocatalytic reduction.** The CO $_2$  photocatalytic reduction experiments were carried out in a home-made Pyrex reactor with 200 mL volume. A 300 W Xe arc lamp without a filter was used as the light source during the photocatalytic reaction. Typically, 50 mg sample was uniformly dispersed on the bottom of the reactor with a base area of 34 cm $^2$ . Before irradiation, the reactor was blown with N $_2$  for 30 min to remove air and ensure that the reaction system was under anaerobic condition. To avoid bringing other impurity gas in the gas-closed system during introducing CO $_2$  gas process, CO $_2$  and H $_2$ O vapor were in-situ generated by the reaction of NaHCO $_3$  (0.12 g, introduced into the reactor before seal) and HCl aqueous solution (0.25 mL, 4 M) which was introduced into the reactor by syringe. 1 mL of gas was taken from the reaction cell and then was analyzed by a gas chromatograph (GC-2014C, Shimadzu, Japan) equipped with a flame ionized detector (FID) according to the standard curves. Blank experiments were carried out in the absence of CO $_2$  or light irradiation to confirm that CO $_2$  and light were two key influencing elements for photocatalytic CO $_2$  reduction. Control experiments were also used to verify whether the carbon resource was derived from CO $_2$  or catalyst itself.

**Photoelectrode Fabrication and Electrochemical Analysis.** The electrochemical

properties of catalyst samples were examined using electrodes fabricated as follows. 0.1 g of photocatalyst was mixed with 0.04 g of polyethylene glycol (PEG, molecular weight: 20 000) and 2 mL of anhydrous ethanol, and then grounded to form a slurry by agate mortar and pestle. And then, a doctor blading technique was employed to ensure the same thickness for each photoelectrode. The slurry was coated onto a pre-cleaned 2 cm × 1.2 cm fluorine-doped tin oxide (FTO) glass substrate. After air-drying, the prepared electrodes were annealed at 450 °C for 30 min with a heating ramp of 5 °C/min in air to improve the adhesion. The electrochemical properties were performed in a conventional three-electrode cell using an electrochemical analyzer (CHI-660C, Shanghai Chenhua, China). The working electrode was immersed in a sodium sulfate electrolyte solution (0.5 M), using a Pt wire and Ag/AgCl electrode as the counter and reference electrodes, respectively. The working electrodes have an active area of ca. 0.5 cm<sup>2</sup>. For Mott–Schottky experiments, the perturbation signal was 10 mV with the AC frequency at 1 kHz. All the potentials reported here are relative to Ag/AgCl unless otherwise stated. The obtained potentials versus Ag/AgCl was converted to the reversible hydrogen electrode (RHE) according to the equation

$$E_{RHE} = E + 0.212 \quad (1)$$

Where  $E_{RHE}$  is the potential vs. RHE,  $E$  is the measured potential vs Ag/AgCl.

**Theoretical calculation:** The theoretical calculation is performed based on ab initio density function theory (DFT). Exchange-correction effects were taken into account by using the GGA (generalized gradient approximation) function of PBE (Perdew, Burke and Ernzerhof). The band structure and the density of states calculation were performed using the CASTEP code program package, which utilized pseudo-potentials to describe electron-ion interactions and represented electronic wave functions using a plane-wave basis set. The kinetic energy cutoff was set at 400 eV. The Brillouin-zone sampling was performed by using a k-grid of 4×4×1 points for the calculations.

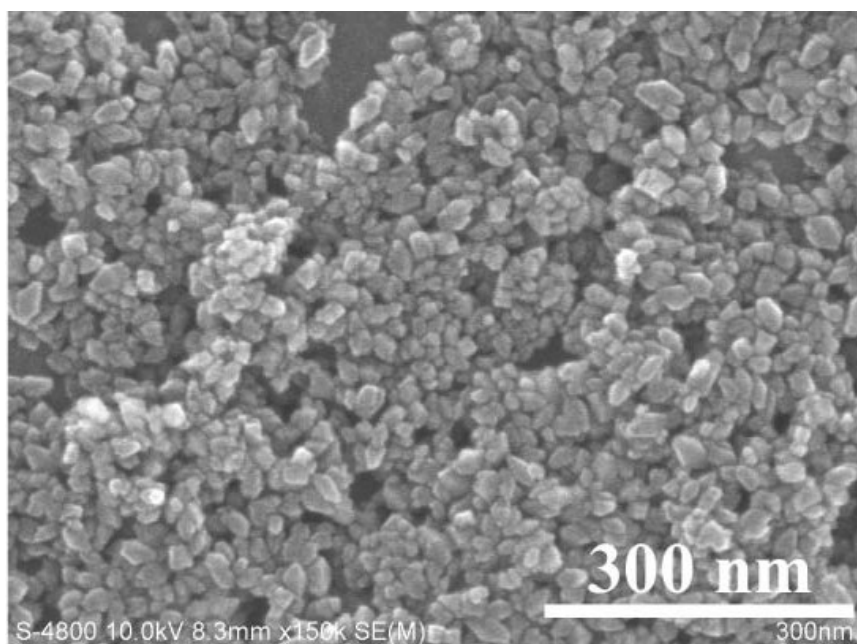


**Fig. S1** SEM images of TW samples

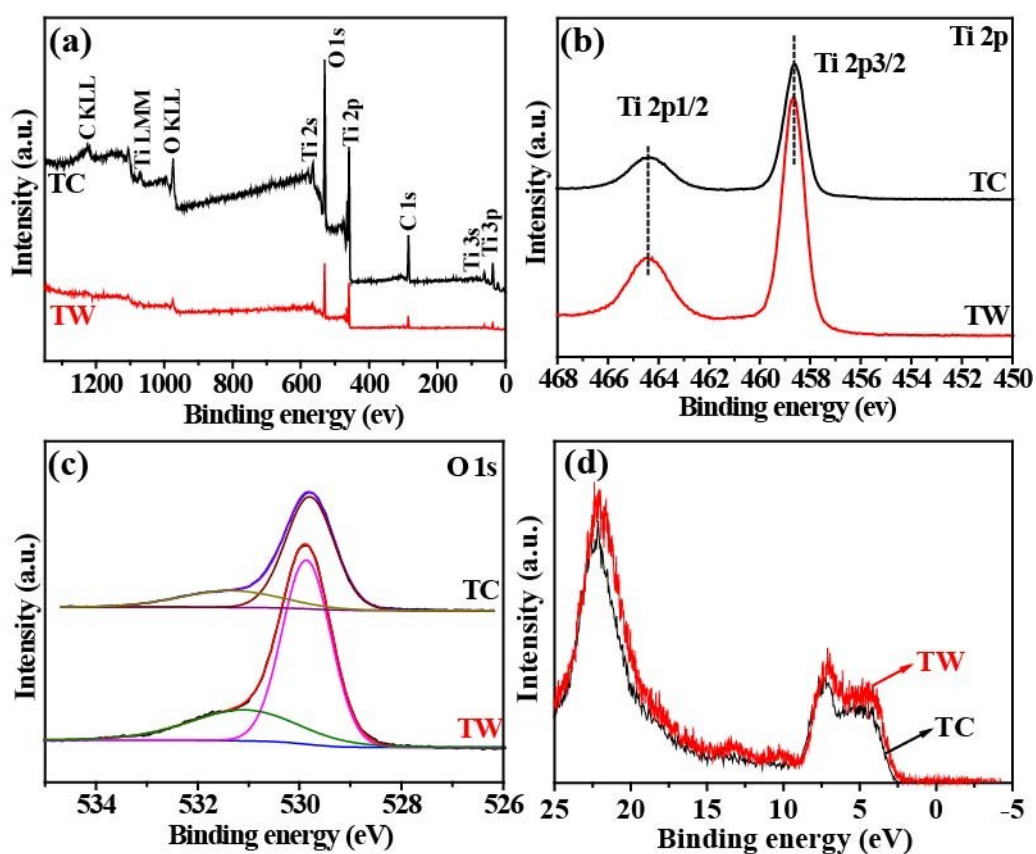


**Fig. S2** XPS spectra of TC and TW samples. Survey (a), High-resolution XPS spectra of Ti 2p (b) and O 1s (c), Valence band (d).

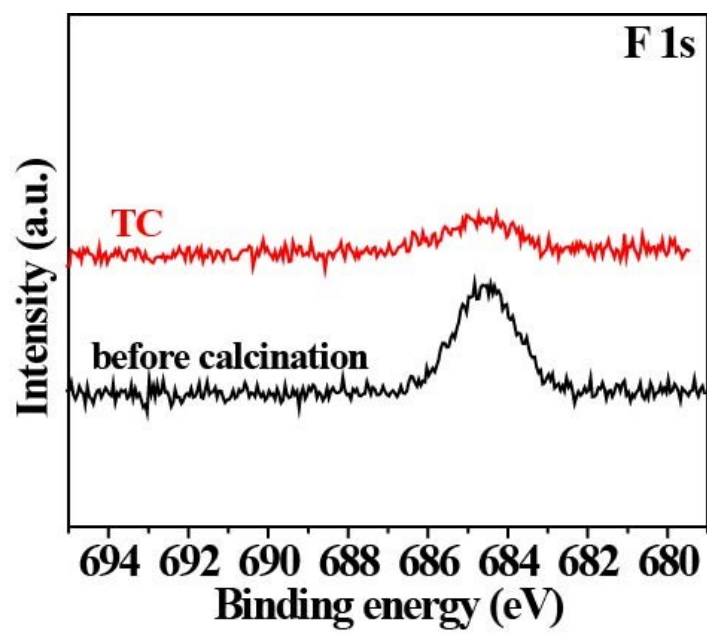


**Fig S3.** F 1s High resolution XPS spectra of TC and the uncalcinated TC samples

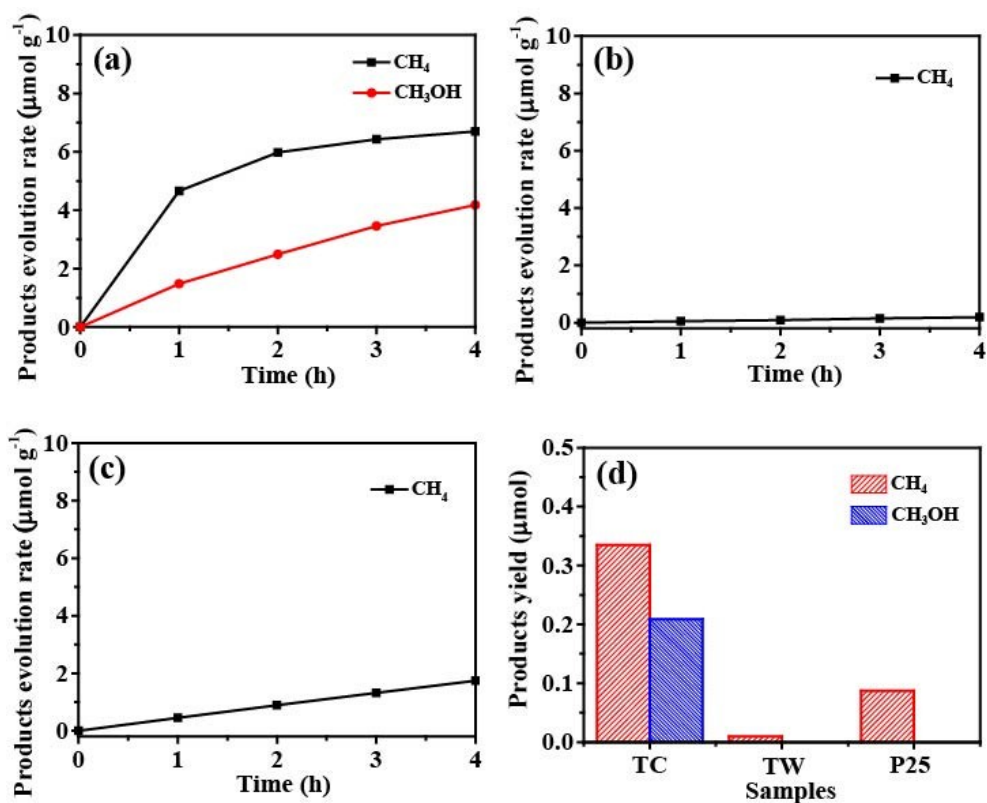


**Fig S4.** Products evolution rate on TC (a), TW (b) and P25 (c), products yield over TC, TW and P25 samples under simulated solar irradiation for 4 h.

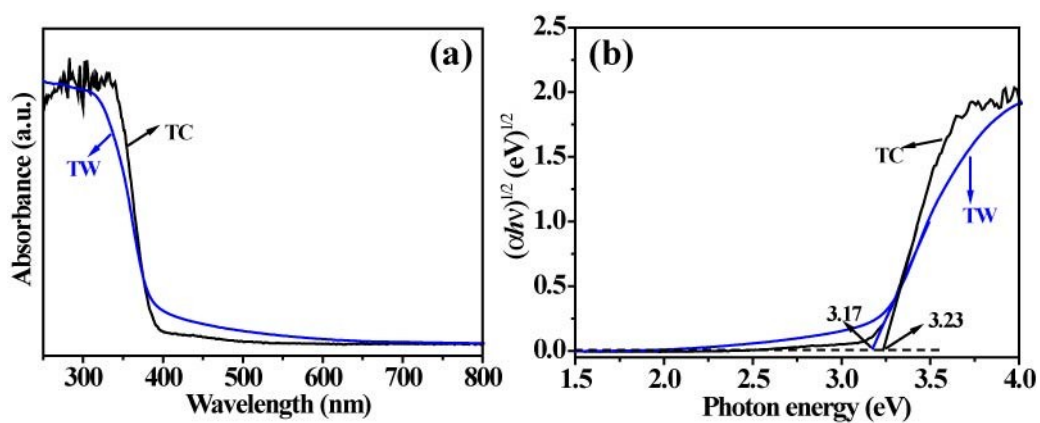


**Fig. S5** UV-Vis diffuse reflectance spectra of TC and TW (a) and the corresponding plots of transformed Kubelka-Munk function versus the energy of photon (b).